FINAL REPORT 8/15/00 - 8/14/04

Contract No. DE-FG0200ER54608

"Fundamental Surface Reaction Mechanisms in Fluorocarbon Plasma-Based Processing "

G. S. Oehrlein
Materials Science and Engineering & Institute for Research in Electronics and Applied Physics
University of Maryland, College Park, MD 20742-2115

H. M. Anderson and J. L. Cecchi
Department of Chemical and Nuclear Engineering, The University of New Mexico, Albuquerque, N.M

D. Graves
Department of Chemical Engineering,
University of California, Berkeley, CA 94720-1462

Contents

A Overview and Highlights 2
B Characterization of CF, CF_2 and COF_2 Densities During SiO_2 and Si Etching in C_4F_8 /Ar 3
C Characterization of Surfaces During SiO_2 and Si Etching in C_4F_8 /Ar 4
D Important Product Species During Etching of SiO_2 4
E Detailed Measurements on Heating and Loss Mechanisms of CF Radicals 5
1. Time evolution of CF_2 rotational temperature 5
2. CF Loss Mechanism 6
3. CF_2 loss in the afterglow 7
4. Decay Time Constant of [F] and [H] in the Afterglow 9
F Vacuum Beam Studies of Plasma Surface Interactions 10
G Molecular Dynamics Simulations of Fluorocarbon Plasma/Surface Interactions 10
References citing support from contract DE-FG0200ER54608. 12
Presentations of Research Supported Under this Grant: 13
US Patent Application 14

A Overview and Highlights

This report provides a summary of results obtained in research supported by contract " Fundamental Surface Reaction Mechanisms in Fluorocarbon Plasma-Based Processing" (Contract No. DE-FG0200ER54608). In this program we advanced significantly the scientific knowledge base on low pressure fluorocarbon plasmas used for patterning of dielectric films and for producing fluorocarbon coatings on substrates. We characterized important neutral and ionic gas phase species that are incident at the substrate, and the processes that occur at relevant surfaces in contact with the plasma. The work was performed through collaboration of research groups at three universities where significantly different, complementary tools for plasma and surface characterization, computer simulation of plasma and surface processes exist. Exchange of diagnostic tools and experimental verification of key results at collaborating institutions, both experimentally and by computer simulations, was an important component of the approach taken in this work.

The panel in the center of figure 1 shows schematically the problem of plasma-surface interactions. Ions, and neutral radicals interact with a surface, and produce a modified surface layer, and stimulate fluxes of neutral products to leave the surface [the effect of electrons and photons on surface processes is ignored]. To describe plasma surface interactions, quantitative measurements of the different neutral fluxes are required, along with a measurement of the total ion flux, decomposition of the ion flux, and measurements of the ion energy distribution as a function of process conditions. Quantification of radical heating (radical temperatures) and loss rates of radicals are also required. In addition, surface chemical characterization is needed.

Several selected results that were obtained in the course of this work on the problem of fluorocarbon discharges interacting with SiO_2 and Si surfaces during etching are shown in Fig. 1. These include the density of fluorocarbon radicals as a function of %Ar in C_4F_8/Ar discharges for given operating conditions, results of compositional analysis of the ion flux, the ion energy distribution function for CF^+ ions as a function of RF bias applied to the substrate, chemical changes of the substrate induced by the plasma-surface interactions, quantitative fluxes of incident species and the evolving flux of substrate species based on measured etching rates. These data are representative, and the total of the data enables us to produce a composite rather detailed picture of key processes in the fluorocarbon-based etching of SiO_2. Additional beam measurements and computer simulations support the conclusions drawn from these studies.

We initially list several progress highlights. This is followed by a more extended description of selected research accomplishments. A list of publications acknowledging support under this grant is presented at the end.

- The first detailed studies of the evolution of the temperature of fluorocarbon radicals and the loss mechanism of CF and CF_2 fluorocarbon radicals in fluorocarbon plasmas without substrate biasing was studied using IR laser diode absorption measurements and pulsed fluorocarbon discharges[i, ii].
- Joint experiments between UNM/UMD enabled quantitative measurements of CF, CF_2 and COF_2 radical concentrations during etching of SiO_2 and Si using industrially important $C_4F_8/Ar/O_2$ gas mixtures as a function of RF bias voltage (ion energy) in two inductively coupled plasma reactors [iii, iv]. This was done both at the University of New Mexico, Albuquerque, and subsequently at the University of Maryland, College Park (UMD), after transporting the IR laser diode absorption measurement equipment to UMD. This work established that CF_2 is by far the dominant FC radical measured for $C_4F_8/Ar/O_2$ discharges (at least by a factor of 10x greater than CF). This work established for the first time a *CF_2 loading effect*. This refers to a significant change of the gas phase CF_2 concentration as the RF bias at an SiO_2 or Si substrate was changed, and etching of these materials was initiated. As the substrate bias is increased and Si and SiO_2 etching commences, the CF_2 concentration in the gas phase is reduced.
- When measuring the abundance of CF, CF_2 and CF_3 at Si and SiO_2 surfaces as a function of process conditions using x-ray photoemission spectroscopy, we also observe a strong decay of CF_2 at the Si

and SiO_2 surfaces during etching for high ion/neutral flux ratios [v]. For discharges with a low ion/neutral flux ratio this is not seen. The gas phase and surface characterization data are in agreement with an important role of CF_2 in the etching process via adsorption on the surface, fluorocarbon film formation, and subsequent ion-induced reaction with the substrate to produce volatile species.

- Our search for important etch products for SiO_2 etching using C_4F_8/Ar discharges indicates that SiF_2 and CO are the dominant Si- , C-, and O-related gas phase etch products for the ion-driven SiO_2 etching process [vi]. For this work, IR laser absorption measurements of CO were complemented by UV-Vis absorption measurements of SiF_2.
- Our work resulted in the most detailed understanding of ion-induced transport of fluorine in surface reaction layers during plasma processing to date, based on both experimental measurements and molecular dynamics simulation [vii],[viii]. Our experimental work showed that argon ions (Ar^+) in fluorocarbon-argon plasmas induce de-fluorination of fluorocarbon surface films, ion driven transport of F from the surface through the surface films and reaction with underlying silicon to form etch products containing SiF_x. Molecular dynamics simulations confirmed these ideas, and provided additional details of the mechanisms involved. These studies are an excellent example of the ways in which simulations and experiments are complementary and illustrate how each brings essential elements to our overall understanding of the process.
- A beam apparatus for experimental simulation of plasma-surface interactions was constructed and initial studies have been completed.
- Both experimental and modeling studies of the effects of magnetic fields on fluorocarbon discharges were completed [ix],[x]. In addition, the impact on gas phase and surface chemistry of adding different noble gases (He, Ne or Ar) to fluorocarbon discharges was studied and published [xi].

B Characterization of CF, CF_2 and COF_2 Densities During SiO_2 and Si Etching in C_4F_8 /Ar

The work at UMD focused on characterization of fluorocarbon-based SiO_2 and Si etching processes. An inductively coupled plasma (ICP) etching reactor was used. This ICP reactor is equipped with numerous diagnostics, and is likely one of the best-characterized and modeled reactors available today. The plasma is produced using 13.56 MHz power, and a SiO_2-coated silicon wafer (125 mm diam.) is located 7 cm downstream from the plasma source and mounted on an electrostatic chuck. A variable frequency RF power supply (500 kHz to 40 MHz) is used to bias the wafer. Helium at a pressure of 5 Torr or greater is applied to the backside of the wafer during the experiment to enable efficient temperature control of the wafer.

Figure 2 displays the "apparent" fluxes of CF, CF_2 and COF_2 estimated from the gas phase density measurements as a function of RF bias voltage applied to either a SiO_2 or a Si substrate [xii]. The fluxes were calculated using a translational temperature of 400 K for CF_2, which is based on the rotational temperature measurement described below. Data are shown for a C_4F_8/60% Ar discharge, but qualitatively similar results were also obtained for pure C_4F_8 discharges and other gas compositions (not shown), although the relative fluorocarbon radical loss rate depends on gas composition. As the RF bias voltage is increased, etching of these materials is induced. The measured etching rates are equivalent to the fluxes of SiO_2 or Si shown in Fig. 2. As the etching rates of SiO_2 and Si increase, a reduction of the fluorocarbon radical gas phase density is observed, producing lower apparent fluorocarbon fluxes. The difference in the fluorocarbon radical fluxes for zero bias voltage (no substrate etching) and at a given bias voltage corresponds to the equivalent particle flux lost. The simplest explanation is that this is due to consumption of the fluorocarbon radicals in the etching process. Consistent with this picture, a more significant reduction is seen for a SiO_2 substrate than for a Si substrate, with the SiO_2 etching at a higher rate than the Si substrate. Figure 2 demonstrates that the corresponding loss rates of CF_2 are high enough to explain the observed SiO_2 and Si etching rates, but that the loss rate of CF cannot account for the observed etching rate of SiO_2.

C Characterization of Surfaces During SiO_2 and Si Etching in C_4F_8 /Ar

In Fig. 3 we show carbon 1s x-ray photoemission spectra obtained for SiO_2 and Si surfaces for C_4F_8 and C_4F_8/90%Ar discharges, and either no RF biasing or a RF bias voltage of –125 V applied to the substrate [xiii]. The C_4F_8/90%Ar discharge is characterized by an ion current density that is more than a factor of 2 that measured for a pure C_4F_8 discharge, and the mass flow of C_4F_8 is only a tenth. One may expect that the much greater ion/neutral flux ratio of a 90% Ar/C_4F_8 discharge will affect the nature of the fluorocarbon layers that is deposited without RF bias as compared to a pure C_4F_8 discharge. The x-ray photoemission spectroscopy data in Fig. 3 obtained with fluorocarbon films produced in either C_4F_8 or C_4F_8/90% Ar do not show a major difference. Both films are highly fluorinated, with the CF_2 group being dominant. Although the fluorocarbon growth rate is dramatically reduced for the C_4F_8/90% Ar discharge, apparently similar species cause FC film growth. The increased inert ion bombardment (at low energy, corresponding to the plasma potential) that results from the much higher ion/neutral flux ratio in the 90%Ar/C_4F_8 discharge apparently does no significantly change the film composition.

When an RF bias is applied to initiate substrate etching, we observe that for pure C_4F_8 discharges the steady-state FC layers that form on etching surfaces remain highly fluorinated. On the other hand, for the C_4F_8/90% Ar discharge a fluorine-deficient steady-state FC film is formed under these conditions (see Fig. 3). The SiO_2 etch rate follows closely the ion current. The enhanced etching of SiO_2 produces a fluorine-deficient steady-state fluorocarbon layer relative to conditions without ion bombardment or the fluorocarbon steady-state layer produced for a pure C_4F_8 discharge. Both a high ion/neutral ratio and high-energy ion bombardment are required to produce fluorine-deficient films important for selective plasma etching of SiO_2 in microelectronic manufacturing.

The dynamic steady-state fluorocarbon layer formed on SiO_2 and Si surfaces during etching enables species that are normally not active etchants of these materials to play an important role in the etching process, e.g. CF_2, after adsorption on the surface and subsequent ion-induced reaction. IR laser absorption measurements performed both in the GEC-ICP Reference Cell at the University of New Mexico, Albuquerque, and the ICP reactor at the University of Maryland, College Park have shown that CF_2 is one of the most abundant radicals in the gas phase, and our XPS surface analysis measurements show a dominance of this group at the surface. We studied the evolution of the gas phase densities of CF, CF_2 and COF_2 as a function of RF bias applied to Si and SiO_2 surface (energy of the bombarding ions), while simultaneously measuring the Si and SiO_2 etching rates to determine the corresponding outgoing fluxes of Si and SiO_2. These data are shown in Fig. 2.

Based on the IR laser absorption work, compositional analysis of the ion flux and calibration of the mass spectrometer data using a Langmuir probe, absolute data on the important radical and ion fluxes are available in this system as a function of processing conditions (see Fig. 4). We find that for the C_4F_8/Ar system the surface fluxes vary from neutral dominated conditions (e.g. the CF_2/ion flux ratio can be greater than 70 in pure C_4F_8) to ion dominated surface flux conditions (for C_4F_8/90% Ar, 70% of the total ion flux is Ar+, and the ion/neutral flux ratio is greater than 1). This variation strongly changes the importance of ion bombardment, ion composition, energy deposition, and neutrals in inducing surface chemical changes during plasma processing.

D Important Product Species During Etching of SiO_2

The focus of the research of Dr. Anderson's group at UNM was on the role of higher molecular weight fluorocarbon (C_xF_y) neutrals, which may be important reactant species for etching clean SiO_2 surfaces, providing there is energetic ion bombardment. Utilizing infrared diode-laser absorption spectroscopy (IRDLAS) and UV-Visible absorption spectroscopy (UV-Vis), They showed that it is possible to make a near complete mass balance of etch reactants and products in an inductively coupled fluorocarbon discharge while actively etching SiO_2 substrates. Langmuir probe measurements were performed to measure the total ion current density. C_2F_4 and CF_2 were shown by IRDLAS to be the main dissociation products in a C_4F_8 plasma discharge. The C_2F_4 concentration decreases as the SiO_2 etching rate increases,

along with CF_2 and CF radicals, suggesting a role in the SiO_2 etching process. The addition of Ar to the C_4F_8 discharge increased the ion flux at the wafer surface, and the consumption rate of C_2F_4 relative to CF_2. The increased ion flux enhanced the SiO_2 etching rate, until at a very high degree of Ar dilution of C_4F_8/Ar the etching rate became neutral limited. They also monitored SiF_2 using UV-Vis absorption and CO by IRDLAS. In their work they found SiF_2 and CO to be the prevalent Si and C gas phase etch products for the SiO_2 etching process [xiv]. Interestingly, the steady-state etching concentrations of SiF_2 and CO had a 1:2 relationship, consistent with stoichiometric etching of SiO_2. Mass balances on the dominant plasma reactants and products under active SiO_2 etching conditions are shown in Figure 5. The behavior of C_2F_4 with respect to CF_2 in both pure C_4F_8 and Ar/C_4F_8 mixtures are shown in figures 6-A and 6-B. It was observed that for fluorocarbon deposition conditions (i.e. bias powers less than 65 W) in pure C_4F_8, the ratio of CF_2/C_2F_4 remained fairly constant around a value of 0.66. At biases above 65 W, the ratio dropped to a value around 0.5, even as the etch yield increased. This suggests that in pure C_4F_8 discharges, CF_2 is the more reactive species in the oxide etch process. In C_4F_8/Ar discharges, the ratio of CF_2/C_2F_4 changes dramatically from that observed in pure C_4F_8 discharges (1.6 compared to 0.55) at the same etch yield, due in part to the more dominant participation of C_2F_4 as a source of etchant material.

E Detailed Measurements on Heating and Loss Mechanisms of CF Radicals

Professor Cecchi's group at UNM undertook a series of measurements to characterize the loss mechanisms of CF_x radicals and F atoms in fluorocarbon plasmas. As seen above, for selective silicon dioxide etching as practiced in semiconductor and related manufacturing, CF, CF_2 radicals are the precursors of the fluorocarbon film[xv] that leads to selectivity, and F atoms participate in the etching process.

Our measurements have been carried out in a commercially-standard inductively coupled plasma (ICP) reactor, utilizing the representative feedstocks of C_2F_6 and CHF_3, in combination with other gases, including Ar, H_2, and O_2. To access kinetic information, we have operated the reactor in a pulsed mode. Our primary diagnostic for [CF_x] measurements has been a wavelength modulated infrared diode laser spectroscopy system[xvi]. This system provides absolute measurements of [CF], [CF_2], and CF_3], utilizing an N_2O reference cell to calibrate for any laser output, window transmission, etc. For the modulated discharges, the data acquisition of the laser system is synchronized with the pulsed plasma providing 100 □s time resolution of the radical concentration measurements. The relative density of F atoms was obtained by time-resolved actinometry, which was facilitated by maintaining a small amount of power on the wafer chuck after the termination of the ICP power pulse. The time resolution for [F] measurements was 1ms.

Previous kinetic studies neglected the transient behavior of the temperatures of the radical species.[xvii,xviii,xix,xx] Measurement of the time-dependent temperature is necessary to determination the absolute concentration of species from the diode laser measurements. As well, the time evolution of the temperature is an important characteristic in its own right. In this work, we have extracted the time-dependent rotational temperature of CF_2 from the time-dependent diode laser measurements. Modeling[xxv] has shown that the rotational and translational temperatures of radicals in a plasma equilibrate in a short time (on the order of a few collision), so we make the assumption that the rotational temperature reflects the translational temperature as well. Details of the measurements are described elsewhere.[xxi,xxii]

1. Time evolution of CF_2 rotational temperature

Dr. Cecchi's group has also measured the CF_2 radical rotational temperature using wavelength modulated diode laser spectroscopy. Rotational temperature is determined by measuring a series of CF_2 absorption features and using the Beer-Lambert law to fit the absorption features to a line, from which rotational temperature can be extracted. The ν1 band $^RQ_8$ CF_2 eo↔oe and ee↔oo rotational lines J=16, 18, 19, 21-23 are used for this measurement. The measurements were done using a 9:1 CHF_3:Ar gas mixture. Our parameter space included ICP source power from 300 to 900W and total pressure from 10 to 30 mTorr, with mean gas residence time held constant at 1 s to facilitate comparison of time constants acquired

under different process conditions. Pulse frequency was varied from 4 to 50 Hz at duty factors from 10 to 50%. Our time resolution was 0.1 ms. A typical rotational temperature time evolution is shown in Figure 7. The process condition is 600 W ICP source power, 20 mTorr total pressure, 1 s mean gas residence time, and 9:1 CHF_3:Ar chemistry. Pulse frequency is 10 Hz with 25% duty factor. The plot includes the rotational temperature data as well as a line fitted to the data assuming first order rise and decay. CF_2 rotational temperature time evolution is characterized by a first order rise upon plasma ignition to the steady-state temperature of 408 ± 42K. The time constant for this rise is 3.3 ± 1.6 ms. Once the plasma is extinguished, rotational temperature shows first order decay to 295 ± 18K. The time constant for the decay is 13.2 ± 2.8 ms. For pulse frequencies from 4 to 20 Hz, the rotational temperature exhibits similar time-dependent behavior and the steady state rotational temperatures and the time constants in the rf-on and in the afterglow are summarized in table 1. At pulse frequencies above 20 Hz, the time scale of the pulsing parameters is similar to that of the time constants for rotational temperature rise and decay.

Pressure (mTorr)	Power (w)	Frequency (Hz)	Decay time constant (ms)	Rise time constant (ms)	Steady state T_r in the rf-on period (K)	Steady state T_r in the afterglow (K)
10 to 30	300 to 900	4				
10 to 30	600 to 900	10	13.2±2.8	3.3±1.6	408±42	295±18
10 to 30	300	10				
10 to 30	300 to 900	20	8.0±0.9			

Table 1. A summary of the steady state rotational temperatures and the time constants in the rf-on period and in the afterglow.

2. CF Loss Mechanism

We have found that over a broad parameter space, [CF] shows a first order exponential decay with a time constant that decreases with increasing pressure. This suggests volume recombination as the loss mechanism for CF molecules over this pressure range. In Figure 8, we plot the [CF] decay time constant as a function of collision period, which is calculated assuming a gas mixture with a molecular diameter of 1 Å. This plot shows that the decay time constant is proportional to the collision period. The slope of the line in this plot indicates that a CF molecule undergoes, on average, 184 collisions before it reacts with another molecule or atom to form a new molecule. The plasma contains charged and neutral atoms and molecules comprised of C, F, H, and Ar. CF is likely to collide with many different atoms and molecules before it collides with the atom or molecule with which it reacts to form another molecule.

To further study the decay behavior of [CF], we measured the decay rate under different pressures in the two gas systems, CHF_3 and C_2F_6. As in the previous measurements, linearity between the [CF] decay rate and pressure was found for both systems. Figure 9 shows such an example in CHF_3. To find the possible species with which CF recombines in the afterglow, we assume that it is species A with the following Reaction,

$$CF + A \xrightarrow{k_R} CFA \qquad \textbf{(1)}$$

Where k_R is the reaction rate of the recombination reaction of CF with species A.

The first order decay rate of [CF] comprises three parts: the loss by pumping, the loss by the recombination reaction, and the loss to surfaces,

$$\frac{d[CF]}{dt} = -\left(\frac{1}{\tau} + k_R[A] + k_s\right)[CF] \qquad \textbf{(2)}$$

where the residence time τ is a constant. The loss rate to surfaces k_s is also a constant based on the previous studies in our group.[xxi] From equation (2), the total decay rate of [CF] in the afterglow should have a linear relationship with the density of species A, with which CF recombines.

Taking into consideration of the transient behavior of species A, we evaluate the rate equation at t=0, where the plasma extinguishes, the following equation is obtained,

$$\left.\frac{d[CF]}{dt}\right|_{t=0} = -\left(\frac{1}{\tau} + k_R[A]_0 + k_s\right)[CF] \qquad (3)$$

The initial decay rate on the left of the above equation was measured in the two gas systems with addition of H_2 or O_2 to change the composition of the plasmas. Steady state [CF] and [CF_2] were measured by diode laser absorption spectroscopy and relative [H], and [F] were obtained by optical emission spectroscopy. The transitions used in optical emission spectroscopy include F at 703.7 nm, H at 656.3 nm, and Ar at 750.4 nm. The emission intensity ratio of the Ar line at 750.4nm to the Ar line at 811.5nm is monitored and the electron temperature of the hot electrons does not change with tool parameters in the range explored in this work

.

We found the linear relationship between the initial decay rate of [CF] and the relative [F] in both systems. Figure 10 shows such a relationship in CHF_3. The point in the figure with error bars is for the case without any addition of H_2 or O_2. The figure also shows that the [CF] decay rate decreases with the addition of H_2 and increases with the addition of O_2. The linear relationship between the decay rate of [CF] and the relative density I_F / I_{Ar} suggests that F may be the species with which CF recombines in the gas phase. The part below the dashed line in the figure represents the sum of the loss by surface processes and by pumping. The value is 59 s^{-1}. The part above the dashed line is due to the loss by the recombination reaction. That the line does not start from the origin suggests the presence of other excitation paths other than the direct excitation from the ground state for F in our plasmas.

3. CF_2 loss in the afterglow

After the plasma extinguishes, [CF_2] increases to its maximum value in a few milliseconds.[xxi] The [CF_2] time evolution after the maximum value shows a combination of 2nd order and 1st order losses for the entire range of ICP power and pressure that we investigated. This part of the time evolution data was modeled by the following equation

$$\frac{d[CF_2]}{dt} = -k_2[CF_2]^2 - k_1[CF_2] \qquad (4)$$

where $k_2[CF_2]^2$ represents the loss rate due to the 2nd order loss process, and $k_1[CF_2]$ represents the loss rate due to the 1st order loss process, k_2 and k_1 are the rate coefficients of the 2nd order and the 1st order losses, respectively.

The 2nd order loss process of CF_2 was observed in laser photolysis measurements and was determined to be the following reaction[xxiii,xxiv]

$$CF_2 + CF_2 \xrightarrow{k_2} C_2F_4 \tag{5}$$

The rate equation of this reaction is

$$\frac{d[CF_2]}{dt} = -k_2[CF_2]^2 \tag{6}$$

To study the temperature dependent rate coefficients, the temperature of the reactants must be held constant. The CF_2 rotational temperature shows that the CF_2 rotational temperature decreases to the wall temperature with a decay time constant of 13.2ms. The chamber wall temperature in this study was controlled to be in the range of 24-26°C. Following approximately three time constants (about 40ms), the CF_2 rotational temperature decays by about 95%. So we can reasonably assume that CF_2 rotational temperature decays to its final value of 298K. Since translational temperature and rotational temperature equilibrate with each other within a few collisions,[xxv] the rate coefficients at 298K can be determined.

Solving equation (4) for $[CF_2]$,

$$[CF_2] = \frac{[CF_2]_0}{\exp(k_1 t) + [CF_2]_0 \cdot (k_2 / k_1) \cdot (\exp(k_1 t) - 1)} \tag{7}$$

The rate coefficients k_2 and k_1 were determined by fitting the decay curve of $[CF_2]$ by equation (7). $[CF_2]_0$ represents the CF_2 density at a time when the curve fitting is initiated.

To measure the 2nd order rate coefficient at 298K accurately, any temperature change associated with the heat generated or absorbed by the reaction should be minimized. Thus it is desired to determine the rate coefficient with low $[CF_2]$. In an open system like our ICP reactor, a high gas residence time is required to limit the change in the availability of CF_2 at the path where the absorption measurement takes place due to pumping and the finite volume of the reactor. The highest gas residence time achieved was 5s in CHF_3 plasmas and 2s in C_2F_6 plasmas. Some examples of the curve fitting are given in figure 11. From the well fitted curves (R^2>0.95), the rate coefficients at 298K have been determined and are listed in Table 2. Also listed are the experimental conditions. An ICP source power of 300W was used in all the cases to limit excessive wall heating.

Gas (w/ 10%Ar)	Residence Time (s)	Pressure (mTorr)	k_2 ($\times 10^{-14}$ cm^3s^{-1})	k_1 (s^{-1})
CHF_3	5	10	1.3	0.5
			1.5	0.8
C_2F_6	2	10	1.5	1.1
		50	1.8	2.2
		70	1.6	2.5

Table 2. Experimental conditions and rate coefficients of CF_2 in the afterglow.

The results in the above table indicate that the 2nd order rate coefficients obtained in the two gas systems are close and the rate coefficient shows no dependence on pressure. The average value of k_2 at 298K is $1.5\pm0.2\times10^{-14}$ cm^3s^{-1}. The rate coefficient is in agreement with the result reported by Dalby,[xxiii] which was determined to be $(2.8\pm2.0)\times10^{-14}$ cm^3s^{-1} at 298K. The results by other measurement are larger than our results due to their neglect of the first order loss path or the time-varying temperature.[xxvi,xx,xxiv]

After 40ms into the afterglow, the major species in the reactor are the feed gas molecules and the CF_2 radicals. This excludes the 1st order loss due to any recombination reaction between CF_2 and other species. Then the first order loss rate comprises the pumping loss and the surface losses. The first order loss coefficient is the sum of the two loss coefficients,

$$k_1 = k_{pump} + k_{wall} = \frac{1}{\tau} + k_{wall} \qquad (8)$$

where k_{pump} represents the decay rate coefficient by pumping, k_{wall} is the decay rate coefficient by the surface loss. τ is the residence time for CF_2.

If we assume that the residence time of the CF_2 radicals is the same as the residence time of the feed gas, then the average k_{wall} value is $1.0\pm0.8s^{-1}$. The sticking coefficient of CF_2 in the afterglow is $(8\pm6)\times10^{-3}$ at 298K.

4. Decay Time Constant of [F] and [H] in the Afterglow

A characteristic time evolution of relative [F] and its fitted models are shown in Figure 12. The process conditions include 300W source power, 40W bias power, 10mTorr total pressure and 1s mean gas residence time. The source power was pulsed at 10Hz with a duty factor of 25% while the bias power was sustained continuously. Upon ignition of the plasma, I_F / I_{Ar} increases according to a first order exponential. As the plasma extinguished, I_F / I_{Ar} shows first order exponential decay. The same behavior is true for the entire range of ICP source power and pressure that we investigated. The decay time constant is in the range of 3-7ms.

The time evolution of relative [H] is similar to that of [F] and it shows first order exponential decay. The decay time constant of [H] is 8.7±2.7ms.

F Vacuum Beam Studies of Plasma Surface Interactions

Understanding and controlling reactions at surfaces exposed to reactive plasmas is at the heart of plasma etching and other plasma-based technologies used in semiconductor manufacturing. We have conducted a combined experimental and modeling study of various aspects of this set of complex problems. The experimental system used is a vacuum beam apparatus designed to expose surfaces (silicon and silicon dioxide) to radicals and ions with in-situ measurement of etch or deposition rate. Construction of this apparatus was completed during the course of this project.

The vacuum beam system employed in this study is sketched in Figs. 13 and 14. Figure 14 is a side-view schematic of the system, illustrating the plasma radical source, and the means by which the radical beam is either detected by the threshold ionization mass spectrometer (left image) or may be directed to impact a selected surface (not shown, right image). In this configuration, the mass spectrometer samples species reflected/desorbed from the surface.

The system geometry can be understood more clearly by examining Fig. 14. This figure is a top-view showing the relation between the radical source and an adjacent Ar^+ ion beam and a electron-generating filament. The electron beam is used to neutralize dielectric surfaces (i.e. SiO_2) when the Ar^+ ion beam impacts the surface.

The base pressure of the main vacuum chamber is about 10^{-8} torr, and operating pressure of the external radical source is about 0.5 torr. For the results presented here, the plasma source is operated with a mixture of 94 % argon and 6% C_4F_8. The plasma source is separated from the main chamber by a stage of differential pumping to minimize the gas load on the main chamber. Main chamber pressure during beam operation is less than 10^{-6} torr.

The operation of the system is as follows. First, species leaving the small plasma radical source are characterized with the mass spectrometer in the 'down' position, using methods that have been described in detail previously.[xxvii] Then, after the mass spectrometer is moved out of the way, a quartz crystal microbalance (QCM) is introduced into the chamber with the transfer arm through the loadlock, and is mounted on a sample loading dock, supported by a rotatable feedthrough. The Ar^+ ion beam can be directed to the surface and its energy can be controlled from several hundred eV to 2 keV. Ion current is measured with a Faraday cup. The film deposited on the QCM (Si or SiO_2) is then exposed to the beam of neutral and ion species and the rate of film deposition or etching can be measured. A typical result is shown in Fig 15: the etch yield for 1000 eV Ar^+ ions on either Si or SiO_2 surfaces is plotted as a function of the ratio of total neutral flux to ion flux. This result shows how the etch yield can increase then decrease as this flux ratio increases over this range, implying that neutrals can act as either etch or deposition precursors.

Details of the results of the study using this apparatus are reported in the reference [xxviii]. As summarized in [2], it appears that under the conditions utilized in the study, heavy species (heavier than CF, CF_2 or CF_3) appear to play a dominant role in both deposition of fluorocarbon films in the absence of ion bombardment and etching in the presence of ion bombardment. We note that conditions under realistic plasma etching conditions may not correspond to the conditions studied in the beam system. An important part of the project achievement was in building and understanding the functioning of this complex apparatus. Future studies will take advantage of this knowledge.

G Molecular Dynamics Simulations of Fluorocarbon Plasma/Surface Interactions

The modeling study was based on the use of molecular dynamics simulations of ion and radical interactions with silicon surfaces. The modeling study was focused on the interactions of C, F and Ar^+ on

Si surfaces. In part, this selection of species was due to the availability of interatomic potentials, and in part due to their relevance to fluorocarbon plasmas.

Details of the development of the interatomic potentials and comparison to results from the literature can be found in references [xxix], [xxx], [xxxi]. These studies helped establish the relevance and expected level of accuracy for the simulation results, and were therefore an important part of the study.

The results that bear directly on the mechanisms of fluorocarbon plasma etching are summarized in references [xxxii], [xxxiii], [xxxiv][6-8]. In related experimental studies at UMD, Oehrlein and co-workers proposed several important roles played by argon ions (Ar^+) in fluorocarbon-argon plasma etching: near-surface regions were de-fluorinated and SiF_x bonds were observed. The conclusion was that Ar^+ transported F from the surface through any surface films to react with underlying silicon to form etch products containing SiF_x. The modeling study confirmed these ideas, although the details of the mechanisms involved as revealed by the simulations are complex.

Simulations predict the formation of layered regions near silicon surfaces exposed to CF_x radicals, F atoms and 200 eV Ar^+. Figure 16 shows a side-view and top-view of a typical simulation result after steady state etching has resulted. A single monolayer of F sits on a ~ 1.5 nm thick layer of SiC, with a layer of SiF_x below that, and finally a layer of disordered Si on top of the original crystalline Si layer. Fluorine adsorbs at the top surface and is ultimately transported in the SiF_x layer via Ar^+ ion energy deposition and associated atomic mixing (see Fig. 17). Thus the experimental observations of defluorination and the appearance of SiF_x bonds when etching occurs are consistent with the simulation results. However, the formation of distinct layers and the complex ways in which Si is transported from the underyling crystalline region up through each of the layers to ultimately be removed as an etch product from the surface could not be inferred directly from the measurements.

References citing support from contract DE-FG0200ER54608.

Xi Li, X Hua, L. Ling, G. S. Oehrlein, M Barela, and H.M. Anderson, Fluorocarbon-Based Plasma Etching of SiO_2: Comparison of C_4F_6/Ar and C_4F_8/Ar Discharges, *J. Vac. Sci. & Technol. A*. 20, 2052-2063 (2002).

Xi Li, L. Ling, X. Hua, M. Fukasawa, G. S. Oehrlein, M. Barela, and H. M. Anderson, Effects of Ar and O_2 additives on SiO_2 etching in C_4F_8-based plasmas, *J. Vac. Sci. & Technol. A*. 21, 284-293 (2003).

Xi Li, Li Ling, X. Hua, G. S. Oehrlein, Y. Wang, and H. M. Anderson, "Characteristics Of C_4F_8 Plasmas With Ar, Ne And He Additives For SiO_2 Etching In A Inductively Coupled Plasma (ICP) Reactor", J. Vac. Sci. & Technol. **A 21**, 1955 (2003).

Xi Li, Li Ling, X. Hua and G. S. Oehrlein, Y. Wang, A. V. Vasenkov and M. J. Kushner, "Properties of C_4F_8 Inductively Coupled Plasmas, Part I: Studies of Ar/c-C_4F_8 Magnetically Confined Plasmas for Etching of SiO_2" J. Vac. Sci. Technol. **A 22**, 500 (2004).

A. V. Vasenkov, Xi Li, G. S. Oehrlein, and M. J. Kushner, "Properties of c-C_4F_8 Inductively Coupled Plasmas, Part II: Plasma Chemistry, Reaction Mechanism of Modeling of Ar/c-C_4F_8/O_2 Discharges" J. Vac. Sci. Technol. **A 22**, 511 (2004).

M.E. Littau, M.J. Sowa, and J.L. Cecchi, *J. Vac. Sci. Technol.*, A 20(5), 1603, 2002

"Molecular dynamics simulations of Ar^+-induced transport of fluorine through fluorocarbon films," D. Humbird, D.B. Graves, X. Hua, and G.S. Oehrlein, *Applied Physics Letters*, 84(7), 1073-1075, 2004.

Barela, M.J., H.M Anderson and G.S. Oehrlein, "The Role of C_2F_4, CF_2, and Ions in C_4F_8/Ar Plasma Discharges Under Active Oxide Etch Conditions," submitted to *J. Vac. Sci. & Technol A* (2004).

"Improved interatomic potentials for silicon-fluorine and silicon-chlorine," D. Humbird and D.B. Graves, *J. Chem. Phys.*, 120(5), 2405-2412, 2004.

"Flurocarbon plasma etching of silicon: Factors controlling etch rate," D. Humbird and D.B. Graves, *J. Appl.Phys.*, 96, 65-70, 2004.

"Atomistic simulations of spontaneous etching of silicon by fluorine and chlorine," D. Humbird and D.B. Graves, *J. Appl.Phys.*, in press, 2004.

"Mechanism of silicon etching in the presence of CF_2, F and Ar^+," D. Humbird and D.B. Graves, *J. Vac. Sci. Technol.*, in press, 2004.

"Atomistic simulations of Ar^+ ion-assisted etching of silicon by fluorine and chlorine," D. Humbird and D.B. Graves, *J. Vac. Sci. Technol. A*, submitted, May 2004.

"Vacuum Beam Studies of Fluorocarbon Radicals and Argon Ions on Si and SiO_2 Surfaces," Y. Kimura, J.W. Coburn, and D.B. Graves, *J. Vac. Sci. Technol. A*, submitted, May 2004.

X. Hua, and G.S.Oehrlein, *Role of fluorocarbon radicals and ions in the SiO_2 surface etching mechanism in fluorocarbon-based discharges, to be* submitted to J. Vac. Sci. Technol. A (2004).

Presentations of Research Supported Under this Grant:

Time evolution of fluorocarbon radical concentrations during pulsed oxide etching plasmas in an ICP reactor, INVITED, T.M. Bauer, X. Wu, and J.L. Cecchi, Gordon Research Conference: Plasma Processing Science, Tilton, NH, August 13-18, 2000

Time-Resolved Measurements of Fluorocarbon Radical Concentrations during Pulsed Oxide Etching Plasmas, T.M. Bauer, X. Wu, and J.L. Cecchi, American Vacuum Society, 47th International Symposium, Boston, MA, October 2-6, 2000, PS2-TuA6.

Measurements of Fluorocarbon Radical Kinetics in an ICP Oxide Etch Reactor, Todd M. Bauer, Xiaomei Wu, and Joseph L. Cecchi, American Institute of Chemical Engineering 2000 Annual Meeting, November 12-17, 2000, Los Angeles, CA, Paper 210b.

Time-Resolved CF_2 Rotational Temperature Measurements in Inductively-Coupled Pulsed Plasmas, X. Wu, T.M. Bauer, and J.L. Cecchi, American Vacuum Society, 48th International Symposium, San Francisco, CA, October 28 – November 2, 2001, PS1-TuM3.

Loss Kinetics of CF_x Radicals and F Atoms in the Afterglow of Inductively Coupled Pulsed Plasmas, X. Wu and J.L. Cecchi, American Vacuum Society, 50th International Symposium, Baltimore, MD, November 2-7, 2003, PS-TuM9.

Plasma-Assisted Etching Processes for Dielectric Materials: Technological Challenges and Elementary Processes on Planar Surfaces and in Microstructures, G. S Oehrlein , Invited, 47th International Symposium of the American Vacuum Society, Boston, Oct. 2000.

High Resolution Plasma Etching of Dielectric Films for Silicon Integrated Circuit Technology, G. S Oehrlein , Invited, Ninth International Symposium on Gaseous Dielectrics, Ellicott City, May 2001.

Pattern Transfer into Dielectric Films by High-Resolution Plasma Etching Techniques, G. S Oehrlein , Invited, The Sixth International Symposium on Sputtering & Plasma Processes, Kanazawa, June 2001.

Current Issues in Pattern Transfer into Dielectric Films by High-Resolution Plasma Etching Techniques, G. S Oehrlein , Invited, 200th Meeting of the Electrochemical Society, Philadelphia, May 2002.

Plasma-Surface Interactions of Nanoporous Silica During Plasma-Based Pattern Transfer Using C_4F_8 and C_4F_8/Ar Gas Mixtures, X. Hua and G. S Oehrlein, Invited, 31st IEEE International Conference on Plasma Science, Baltimore, June 2004 (presented by Ph.D. student X. Hua).

D. Graves, Plasma-Surface Interactions in Plasma Processing, Invited Speaker, 15th International Symposium on Plasma Chemistry, Orleans, France, July 9-13, 2001.

D. Graves, Modeling of Plasma Transport and Surface Interactions, Invited Speaker, International Conference on Phenomena in Ionized Gases, Nagoya, July 16-29, 2001.

D. Graves, What is Known and Not Known About Surfaces Exposed to Plasmas, Invited Speaker, International Workshop on Basis for Low Temperature Plasma Applications, Hakone, Japan, July 23-25, 2001.

D. Graves, Atomistic Simulations of Plasma-Surface Chemistry and Comparison to Experiment, Invited Speaker, Nano and Giga Challenges in Microelectronics, Moscow, Russia, September 10-13, 2002.

D. Graves, Mechanisms of Surface Modifications via Reactive Plasmas, Invited Speaker, American Institute of Chemical Engineers Annual Meeting, San Francisco, November, 2003.

D. Graves, Multiscale, Damage-Free Plasma-Surface Interactions: Extending the Limits of Device Processing, Invited Speaker, First International Symposium on Optical and Electronic Device Technology for Access Network, Tokyo, December, 2003.

D. Graves, Molecular Dynamics Simulations of Silicon Etching in Argon and Fluorocarbon Plasmas. Invited Speaker, International COE Forum on Plasma Science and Technology, Nagoya, April, 2004.

D. Graves, Molecular Dynamics Simulations of Spontaneous and Ion-Assisted Etching of Silicon, Invited Speaker, International Conference on Plasma Physics, Nice, October, 2004. IVC16/ICSS12/NANO8, Venice, Italy, 2004.

D. Graves, Fundamentals of Plasma-Surface Interactions, Invited Speaker, International Conference on Plasma Physics, Nice, October, 2004.

US Patent Application

US Patent Application 10/913323, filed on Aug. 9, 2004
Assignee – University of Maryland

References

[i] M. J. Sowa, M. E. Littau, V. Pohray and J.L. Cecchi, *J. Vac. Sci. Technol*., A18(5), p2122, 2000.

[ii] M.E. Littau, M.J. Sowa, and J.L. Cecchi, *J. Vac. Sci. Technol.*, A 20(5), 1603, 2002

[iii] Xi Li, X Hua, L. Ling, G. S. Oehrlein, M Barela, and H.M. Anderson, Fluorocarbon-Based Plasma Etching of SiO_2: Comparison of C_4F_6/Ar and C_4F_8/Ar Discharges, *J. Vac. Sci. & Technol. A*. 20, 2052-2063 (2002)
[iv] Xi Li, L. Ling, X. Hua, M. Fukasawa, G. S. Oehrlein, M. Barela, and H. M. Anderson, Effects of Ar and O_2 additives on SiO_2 etching in C_4F_8-based plasmas, *J. Vac. Sci. & Technol. A*. 21, 284-293 (2003).
[v] X. Hua, and G.S.Oehrlein, *Role of fluorocarbon radicals and ions in the SiO_2 surface etching mechanism in fluorocarbon-based discharges, to be* submitted to J. Vac. Sci. Technol. A (2004)
[vi] Barela, M.J., H.M Anderson and G.S. Oehrlein, "The Role of C_2F_4, CF_2, and Ions in C_4F_8/Ar Plasma Discharges Under Active Oxide Etch Conditions," submitted to *J. Vac. Sci. & Technol A* (2004).

[vii] X. Hua, and G.S.Oehrlein, *Role of fluorocarbon radicals and ions in the SiO_2 surface etching mechanism in fluorocarbon-based discharges, to be* submitted to J. Vac. Sci. Technol. A (2004)
[viii] Humbird, D., Graves, D.B., Hua, X., and Oehrlein, G.S., *Applied Physics Letters*, 84(7), 1073-1075, 2004.

[ix] Xi Li, Li Ling, X. Hua and G. S. Oehrlein, Y. Wang, A. V. Vasenkov and M. J. Kushner, "Properties of C_4F_8 Inductively Coupled Plasmas, Part I: Studies of Ar/c-C_4F_8 Magnetically Confined Plasmas for Etching of SiO_2" J. Vac. Sci. Technol. **A 22**, 500 (2004).
[x] A. V. Vasenkov, Xi Li, G. S. Oehrlein, and M. J. Kushner, "Properties of c-C_4F_8 Inductively Coupled Plasmas, Part II: Plasma Chemistry, Reaction Mechanism of Modeling of Ar/c-C_4F_8/O_2 Discharges" J. Vac. Sci. Technol. **A 22**, 511 (2004).
[xi] Xi Li, Li Ling, X. Hua, G. S. Oehrlein, Y. Wang, and H. M. Anderson, "Characteristics Of C_4F_8 Plasmas With Ar, Ne And He Additives For SiO_2 Etching In A Inductively Coupled Plasma (ICP) Reactor", J. Vac. Sci. & Technol. **A 21**, 1955 (2003)
[xii] Xi Li, X Hua, L. Ling, G. S. Oehrlein, M Barela, and H.M. Anderson, Fluorocarbon-Based Plasma Etching of SiO_2: Comparison of C_4F_6/Ar and C_4F_8/Ar Discharges, *J. Vac. Sci. & Technol. A*. 20, 2052-2063 (2002)
[xiii] X. Hua, and G.S.Oehrlein, *Role of fluorocarbon radicals and ions in the SiO_2 surface etching mechanism in fluorocarbon-based discharges, to be* submitted to J. Vac. Sci. Technol. A (2004)
[xiv] Barela, M.J., H.M Anderson and G.S. Oehrlein, "The Role of C_2F_4, CF_2, and Ions in C_4F_8/Ar Plasma Discharges Under Active Oxide Etch Conditions," submitted to *J. Vac. Sci. & Technol A* (2004).

[xv] M. J. Sowa, M. E. Littau, V. Pohray and J.L. Cecchi, *J. Vac. Sci. Technol*., A18(5), p2122, 2000.

[xvi] M.E. Littau, M.J. Sowa, and J.L. Cecchi, *J. Vac. Sci. Technol.*, A 20(5), 1603, 2002

[xvii] J. P. Booth, G. Cunge, P Chabert, N. Sadeghi, *J. Appl. Phys*., 85(6), 3097, 1998

[xviii] G. Cunge and J. P. Booth, *J. Appl. Phys*., 85(8), 3952, 1999

[xix] C. Suzuki, K. Sasaki, and K. Kadota, *Plasma Chemistry and Plasma Processing*, 21(1), 139, 2001

[xx] B. A. Cruden, K. K. gleason, and H. H. Sawin, *J. Appl. Phys*., 80(2), 915, 2001

[xxi] T. M. Bauer, "Fluorocarbon Radical Measurements in an Inductively Coupled Plasma Reactor", Ph. D dissertation, University of New Mexico, 2001.

[xxii] X. Wu, "Study of Rotational Temperature and Loss Mechanisms of Fluorocarbon Radicals in an Inductively Coupled Plasma Reactor", Ph. D dissertation, University of New Mexico, 2003.

[xxiii] F.W.Dalby, *J. Chem. Phys*. 41, 2297, 1964

[xxiv] F. B. Leclerc, A. P. Smith, G. D. Hayman, T. P. Murrells, *J. Chem. Soc., Faraday Trans., 92, 3305, 1996*

[xxv] P. G. Kistemaker, A. Tom, and A. E. De Vries, *Physics*, 48, 414, 1970

[xxvi] C. Suzuki, K. Sasaki, and K. Kadota, *Plasma Chemistry and Plasma Processing*, 21(1), 139, 2001

[xxvii] Singh, H., Coburn, J.W., and Graves, D.B., *J. Vac. Sci. Technol. A*, Vol. 18, No. 2, Mar/Apr 2000, 299-305.

[xxviii]] Kimura, Y., Coburn, J.W., and Graves, D.B., *J. Vac. Sci. Technol. A*, submitted, May 2004.

[xxix] Humbird, D., and Graves, D.B, *J. Chem. Phys.*, 120(5), 2405-2412, 2004
[xxx] Humbird, D., and Graves, D.B, *J. Appl.Phys.*, in press, 2004a.
[xxxi] Humbird, D., and Graves, D.B, *J. Vac. Sci. Technol. A*, submitted, 2004.
[xxxii] Humbird, D., Graves, D.B., Hua, X., and Oehrlein, G.S., *Applied Physics Letters*, 84(7), 1073-1075, 2004.

[xxxiii] Humbird, D., and Graves, D.B, *J. Appl.Phys.*, in press, 2004b
[xxxiv] Humbird, D., and Graves, D.B, *J. Appl.Phys.*, in press, 2004c

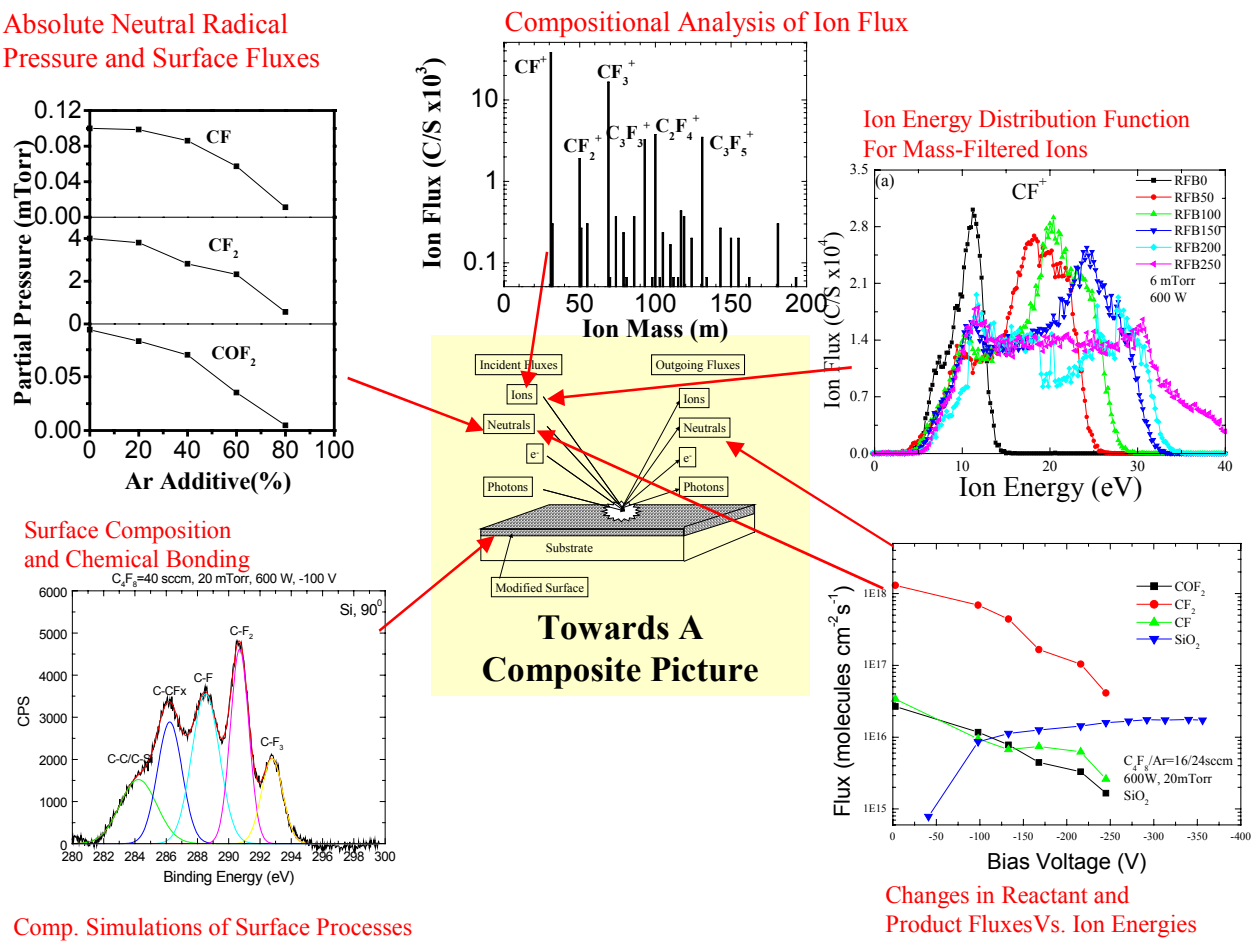


Fig. 1 – Schematic showing application of different experimental measurements performed on plasma reactor to establish properties of C_4F_8/Ar discharges.

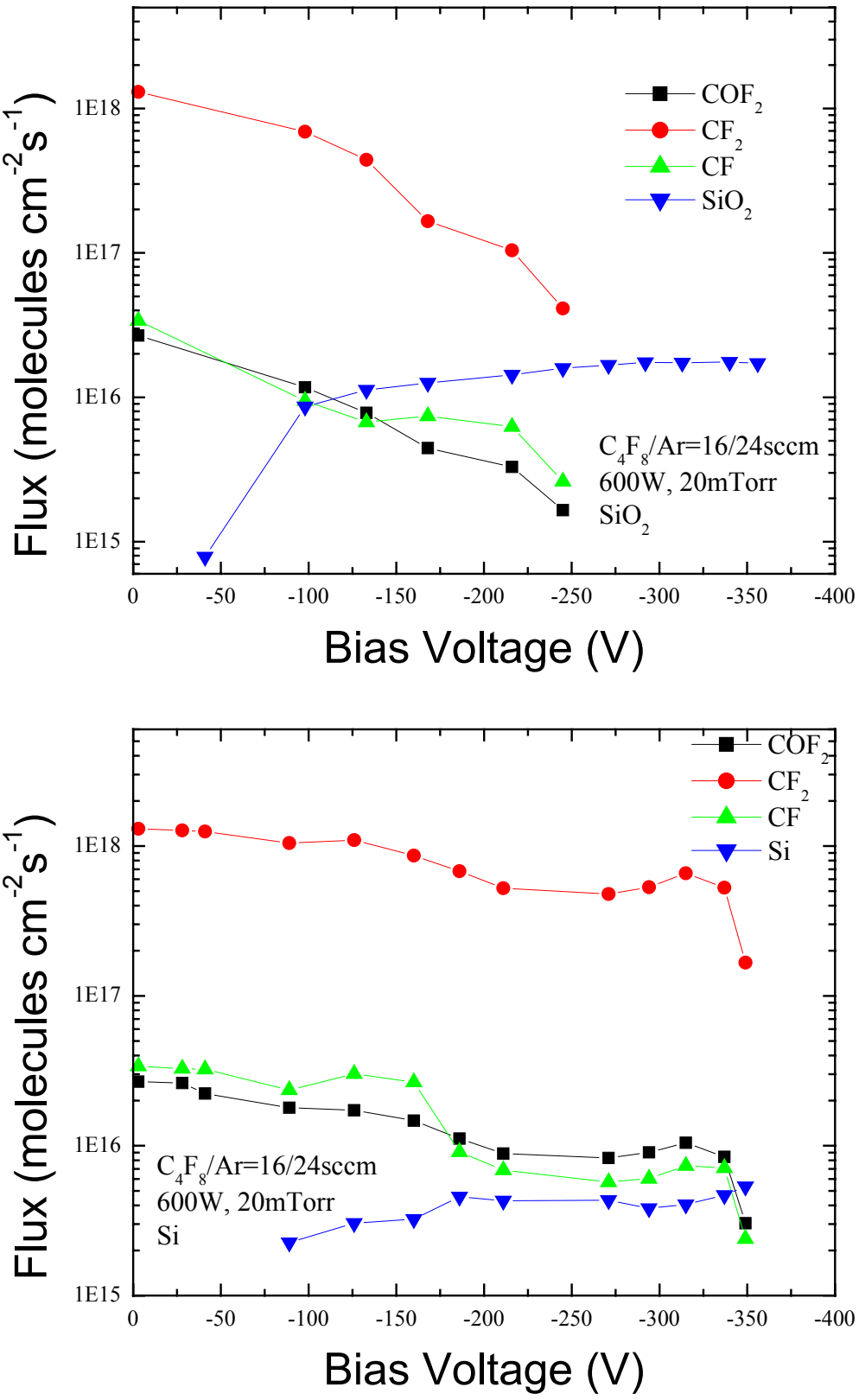


Fig. 2 The variation of the fluxes of CF, CF_2 and COF_2 that correspond to the absolute pressures measured by laser diode absorption vs. RF bias voltage for C_4F_8/60%Ar discharges. Either a SiO_2 (top panel) or Si surface (bottom panel) were in contact with the discharge. The SiO_2 or Si fluxes corresponding to the SiO_2 or Si etching rates measured for the same conditions are also shown.

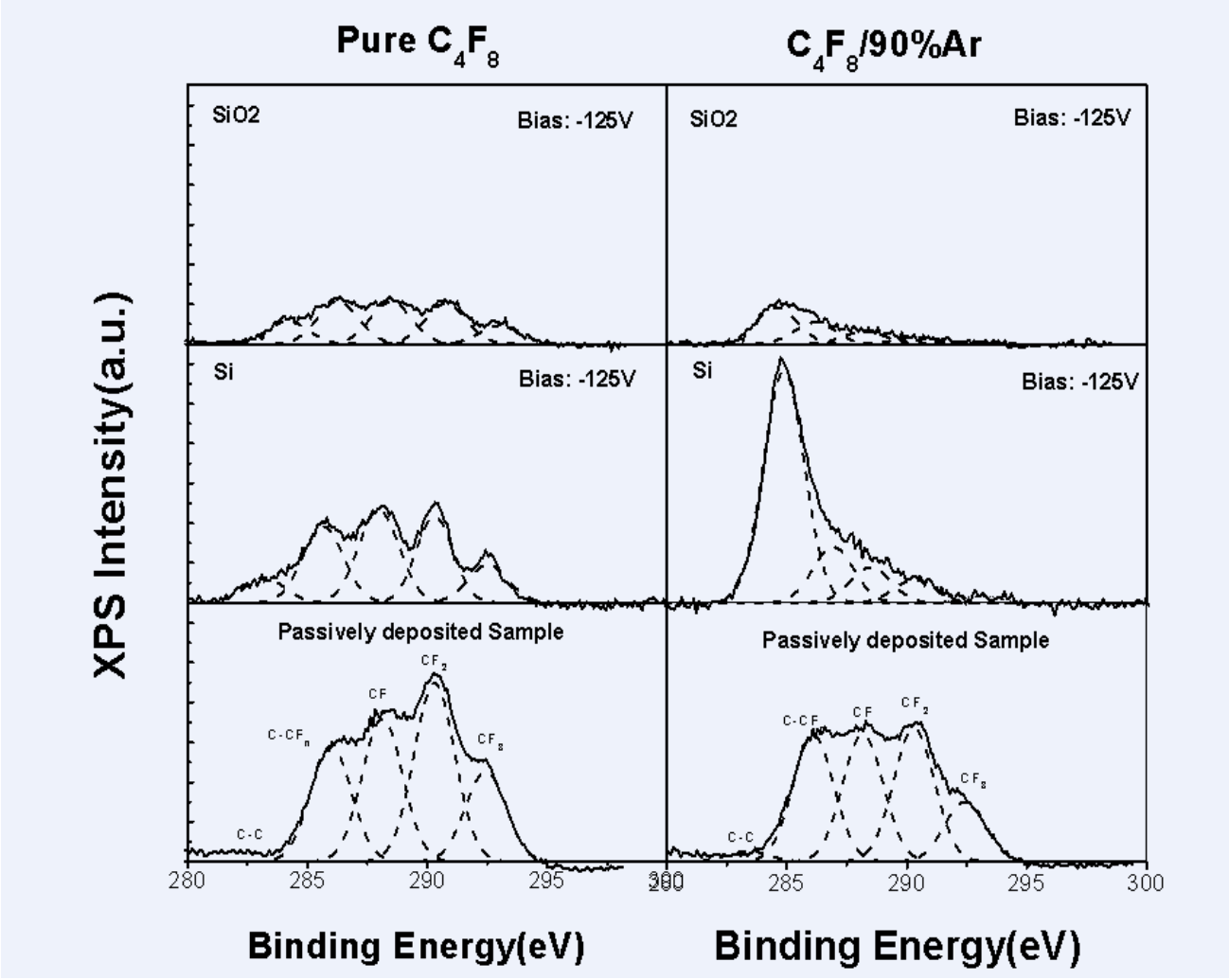


Fig. 3 Carbon 1s spectra of Si and SiO_2 substrates exposed to C_4F_8 or C_4F_8/90%Ar discharges. For the passively deposited films no RF bias was applied and fluorocarbon deposition took place. In the upper panels an RF bias causing a selfbias voltage of -125 V was applied to both Si and SiO_2 substrates, causing etching of these materials underneath a steady-state FC layer. These data show that the FC layer is thicker for the Si substrate, and that both RF biasing and C_4F_8/90%Ar (high inert ion/fluorocarbon radical flux ratio) are required to produce the fluorine-deficient steady-state FC films required for highly selective etching of SiO_2.

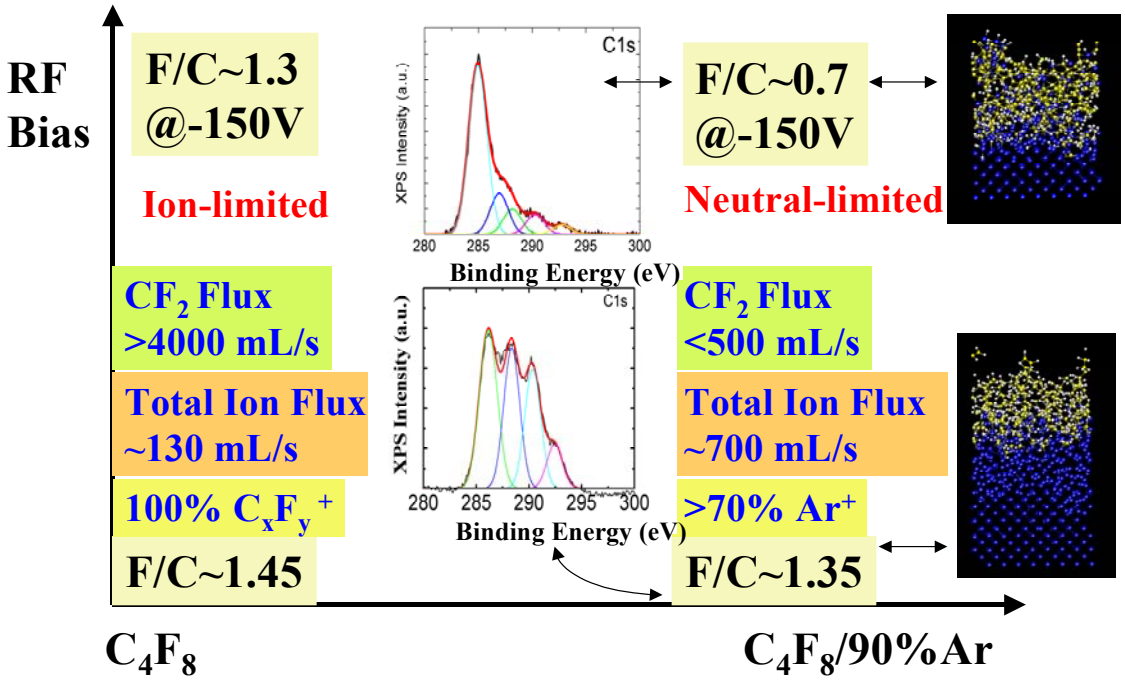


Fig. 4 – Some properties of the C_4F_8/Ar discharges in ICP reactor. In-situ x-ray photoelectron spectra for C_4F_8/90%Ar at two bias conditions, and images of molecular dynamics simulations of these flux conditions are also shown.

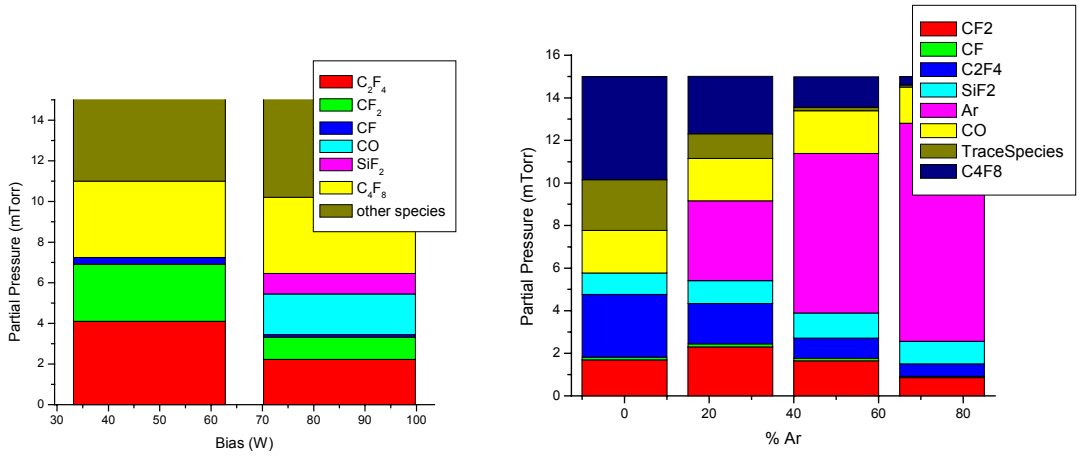


Fig. 5 . Balance of measured species as a function of bias power for pure C_4F_8 and Ar/C4F8 discharges at 350W, 15mTorr total pressure, and 40 sccm.

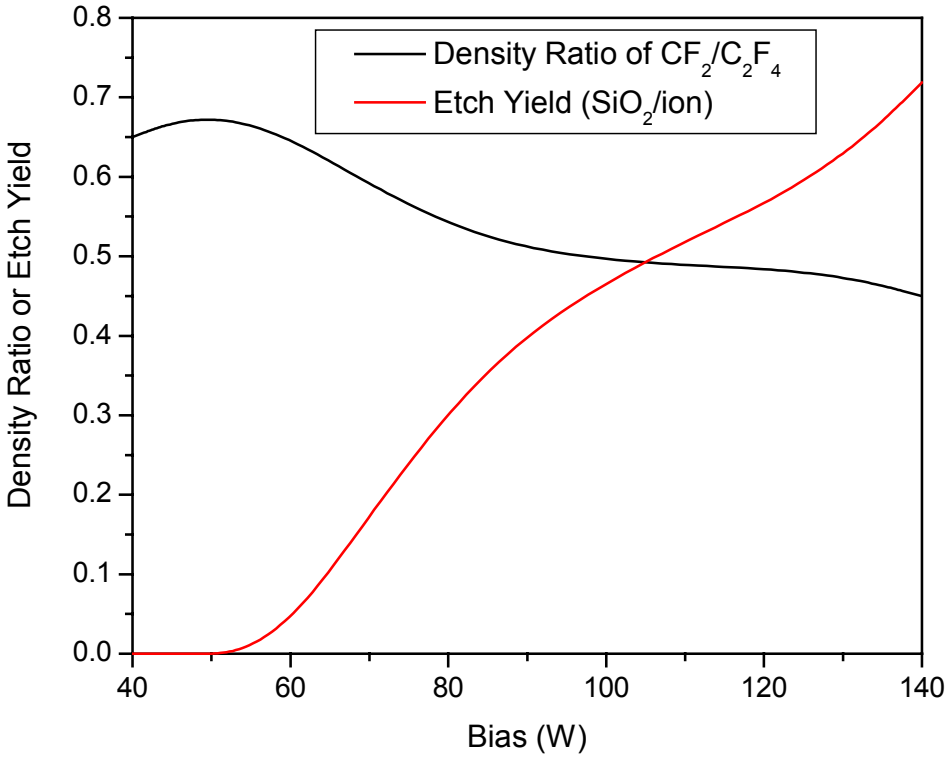


Fig. 6A Plots of the density ratio of CF_2/C_2F_4 and the etch yield as a function of bias power for pure C_4F_8 discharge at 350W, 15mTorr total pressure, and 40 sccm.

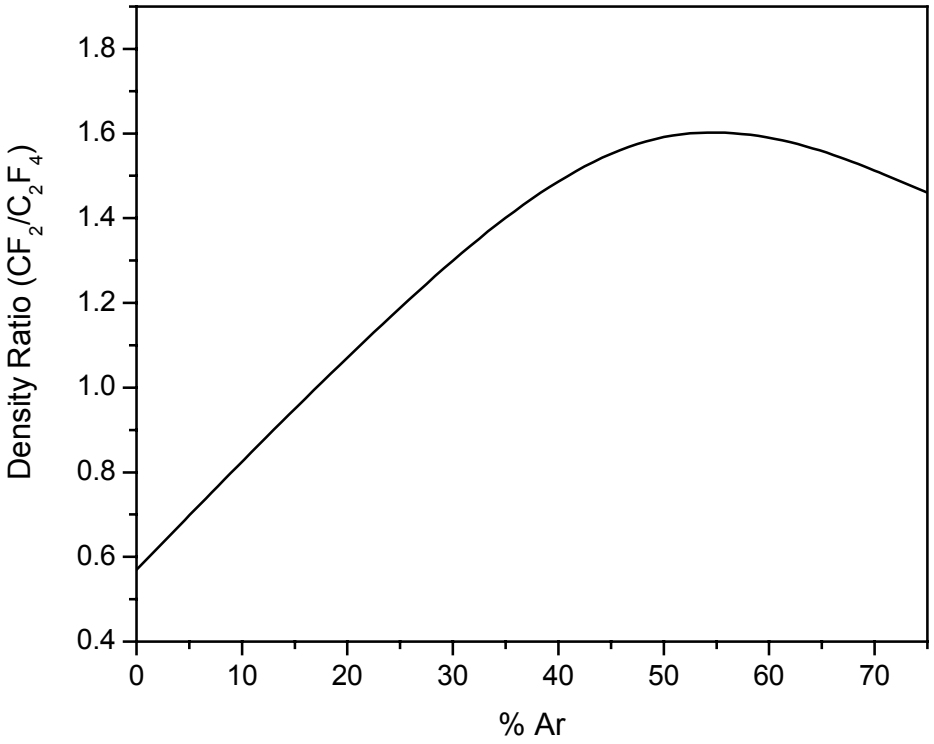


Fig. 6B Ratio of CF_2/C_2F_4 as a function of Ar addition in C_4F_8/Ar at 350W source power, 85W bias,15 mTorr pressure, and 40 sccm.

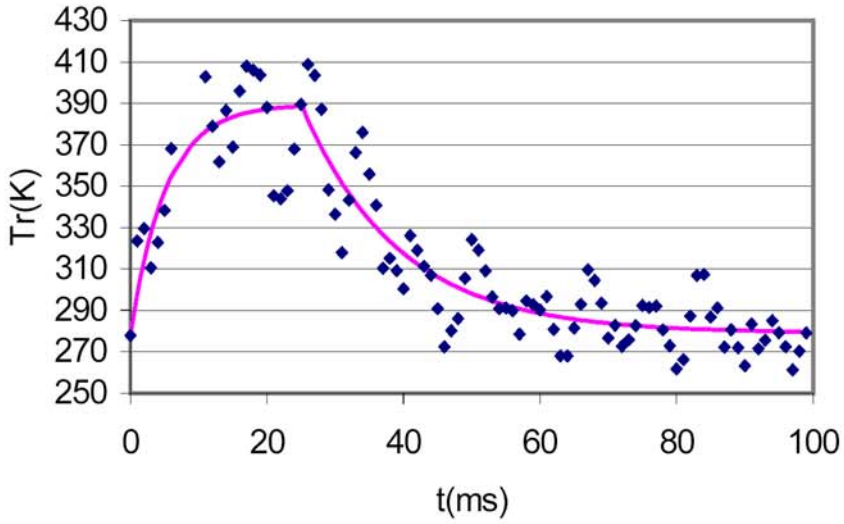


Fig. 7 Rotational temperature time evolution. Process condition is 600 W ICP source power, 20 mTorr pressure, 1 s mean gas residence time, and 9:1 CHF_3:Ar chemistry. Pulse frequency is 10 Hz with 25% duty factor. Fitted line indicates first order exponential rise and decay.

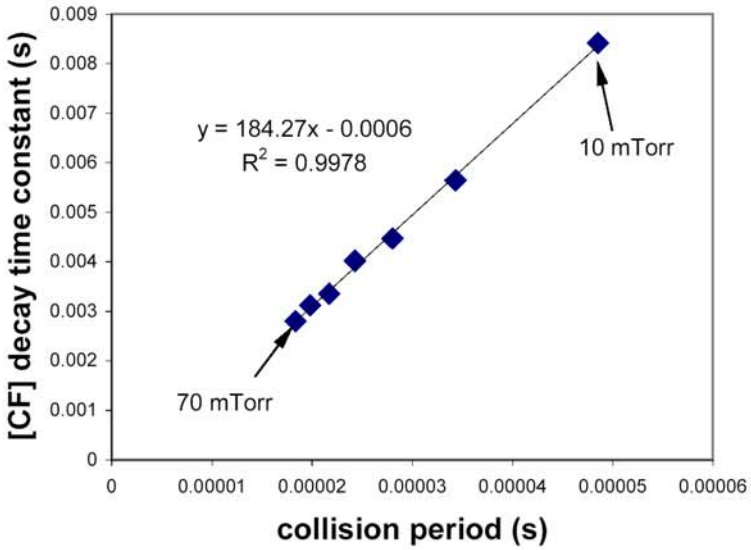


Fig. 8 First order exponential decay time constants plotted as a function of collision period. Process condition is 300 W source power, 10-70 mTorr pressure, and 2 s mean gas residence time.

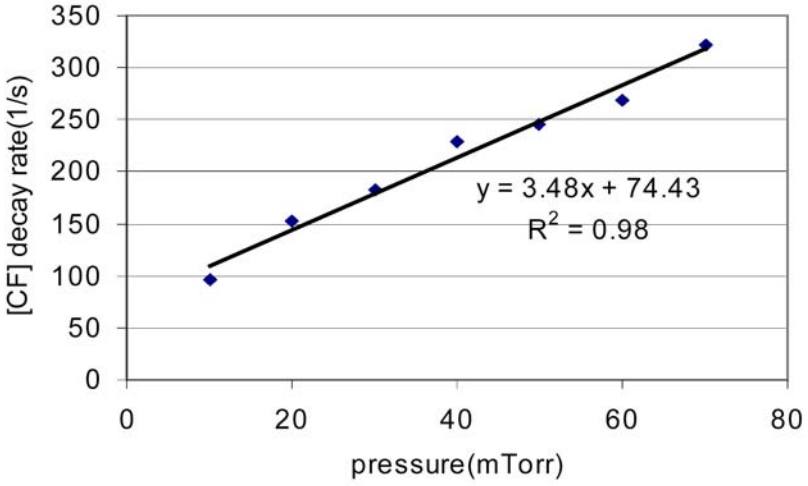


Fig. 9 Decay rate of [CF] in the afterglow as a function of pressure.

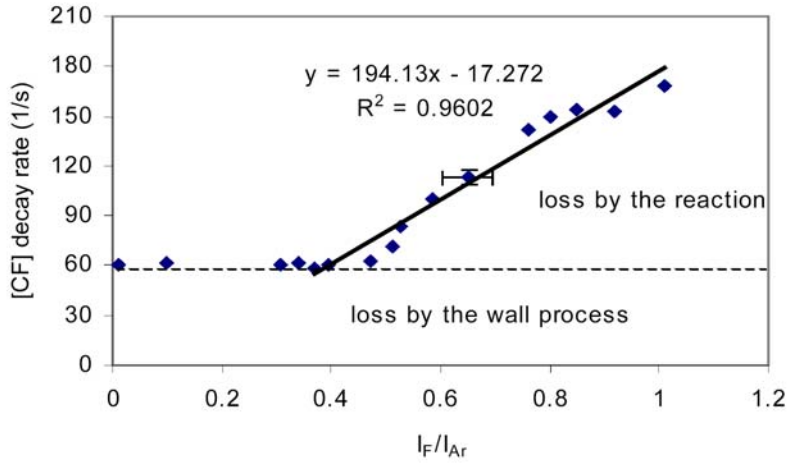


Fig. 10 Decay rate of [CF] versus I_F / I_{Ar} with the addition of H_2 and O_2.

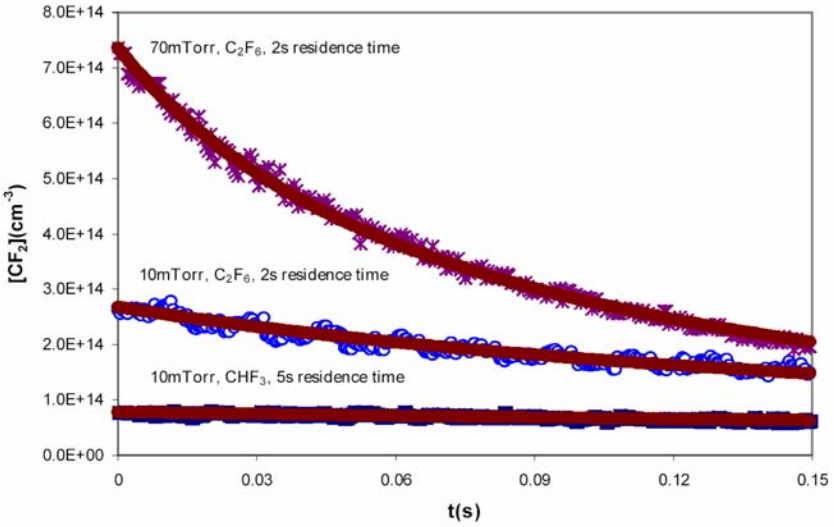


Fig. 11 . Time evolutions of [CF_2] after 40ms into the afterglow for various experimental conditions. The plasmas were pulsed at 4Hz with a duty factor of 0.24. The solid curves represent the least square curve fitting by a combination of 1st and 2nd loss mechanism.

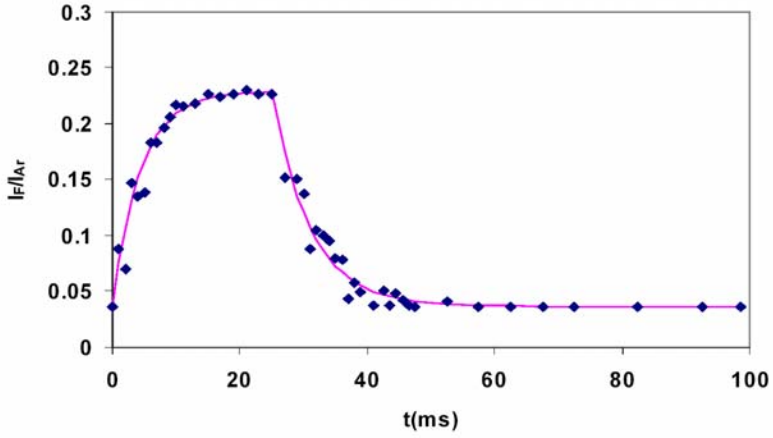


Fig. 12 Time evolution of relative [F].

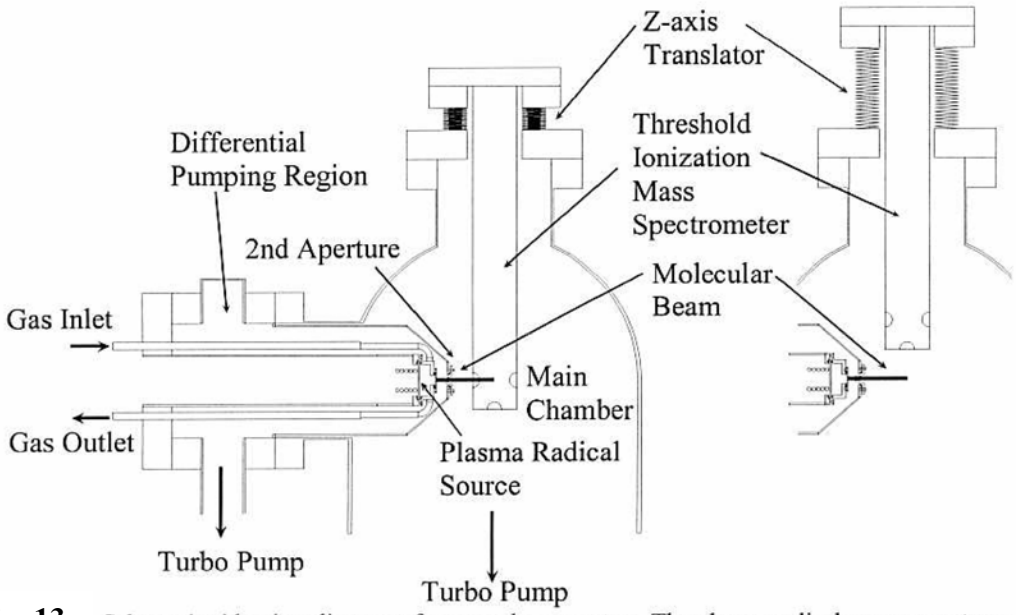


Fig. 13 . Schematic side-view diagram of vacuum beam system. The plasma radical source creates a molecular beam of radicals that may be detected by a positionable mass spectrometer (left), or that are available for interaction with a surface.

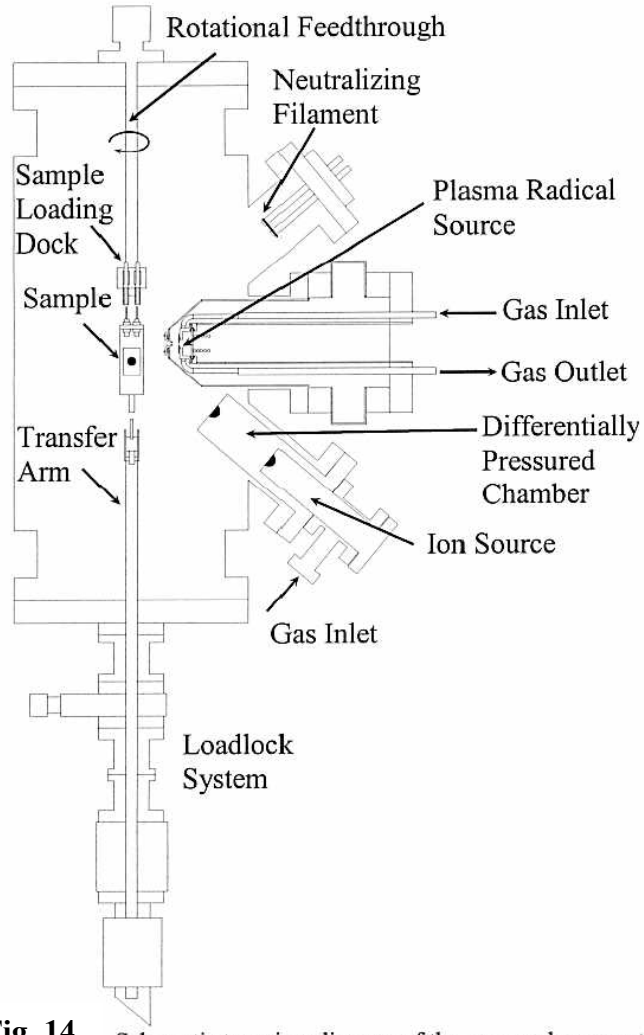


Fig. 14 Schematic top-view diagram of the vacuum beam system, illustrating the relation between the radical source, the ion source, the neutralizing electron-generating filament, the quartz crystal microbalance transfer arm and sample loading dock.

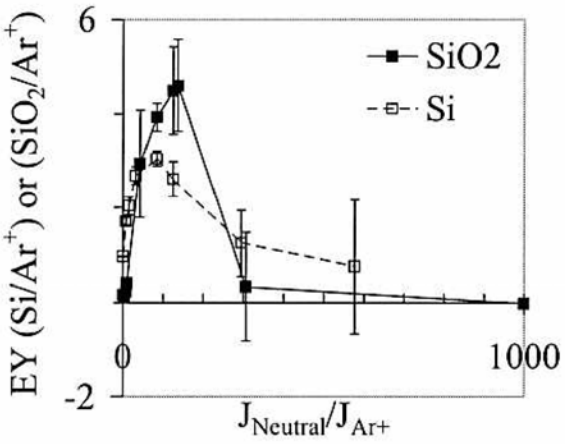


Fig. 15 Plot of measured etch yield (Si or SiO_2 per incident Ar+ ion at 1000 eV) as a function of the total neutral to ion flux ratio.

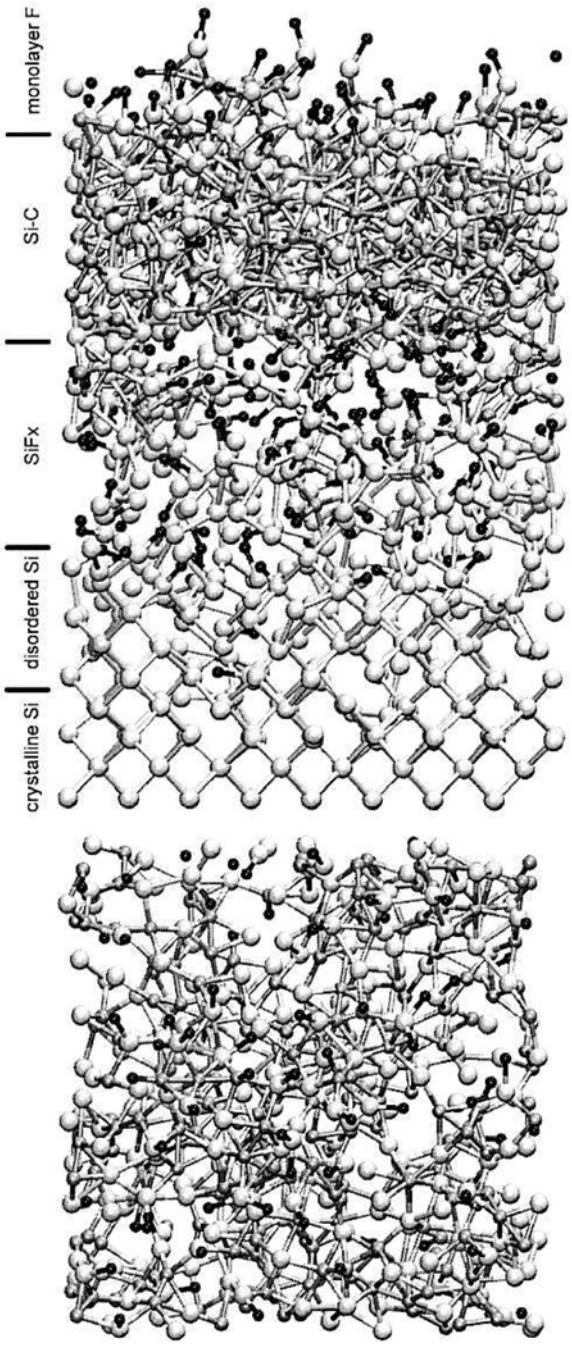


Fig. 16 Top image is the side-view of the near-surface region of silicon exposed to CF_2, F and Ar^+ (200 eV), after steady state etching is achieved. Bottom image is the top-view of this layer. The most striking characteristic is the pronounced layering into a monolayer of F on a relatively thick (~ 1.5 nm) of SiC, above a layer of SiF_x on top of disordered then crystalline silicon. The F in the SiF_x layer originates on the top monolayer and is transported via ion mixing.

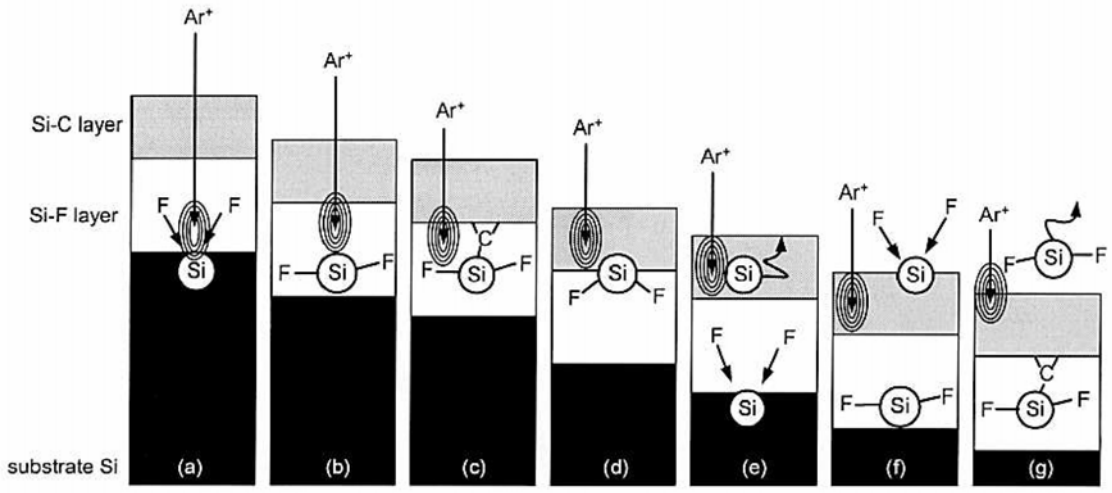


Fig. 17 Schematic of silicon etch mechanism under conditions corresponding to the layered surface shown above. In order to transport Si from the underlying layer, first into the SiF_x layer (a), then into and through the SiC layer (b-f), then finally cause etching, Ar^+ energy deposition must take place throughout the layer.